Received: 3 March 2022 | Revised: 4 July 2022 | Accepted: 22 July 2022
IET Renewable Power Generation
DOI: 10.1049/rpg2.12566
The Institution of Engineering and Technology WILEY

ORIGINAL RESEARCH

Optimal sizing and siting of different types of EV charging stations in a real distribution system environment

Ibrahim Sengor[1,2,3] | **Ayse Kubra Erenoglu**[4] | **Hilmi Cihan Guldorum**[5] | **Ozan Erdinc**[5] | **Akın Taşcıkaraoğlu**[6] | **İbrahim Can Taştan**[7] | **Ali Fuat Büyük**[7] | **João P. S. Catalão**[8]

[1]MaREI Centre, Environmental Research Institute, University College Cork, Cork, Ireland

[2]Department of Electrical and Electronics Engineering, Izmir Katip Celebi University, Izmir, Turkey

[3]School of Engineering, University College Cork, Cork, Ireland

[4]Department of Electrical and Electronics Engineering, Fatih Sultan Mehmet Vakif University, Istanbul, Turkey

[5]Department of Electrical Engineering, Yildiz Technical University, Istanbul, Turkey

[6]Department of Electrical and Electronics Engineering, Mugla Sitki Kocman University, Mugla, Turkey

[7]Smart Systems, R&D, Osmangazi Electricity Distribution Co., Eskişehir, Turkey

[8]Faculty of Engineering, University of Porto and INESC TEC, Porto, Portugal

Correspondence
Ibrahim Sengor, MaREI Centre, Environmental Research Institute, University College Cork, Cork, Ireland.
Email: isengor@ucc.ie

Funding information
Energy Market Regulatory Authority of Turkey (EPDK) R&D Funds; COMPETE; Science Foundation Ireland, Grant/Award Number: 12/RC/2302_P2; Türkiye Bilimsel ve Teknolojik Araştirma Kurumu, Grant/Award Number: 119E215; Fundação para a Ciência e a Tecnologia, Grant/Award Number: POCI-01-0145-FEDER-029803

Abstract
Due to the rising of both economic and environmental concerns in the energy sector, each subdivision of the community is investigating new solutions to overcome this critical issue. For this reason, electric vehicles (EVs) have gained more significance in the transportation sector owing to their efficient and clean operation chance. These improvements, however, bring new challenges such as installation costs, infrastructure renovation, and loading of the existing power system. Here, optimal sizing and siting of EV charging stations (CSs) are examined in a mixed-integer linear programming framework with the aim of minimizing the number of EVCSs in the distribution system (which in turn means to minimize CS-related investment while satisfying EV owners' needs) while satisfying constraints. The proposed optimization model considers EVCS types with different charging rate capabilities to provide opportunities for demand-side management. Moreover, the model takes the actual behaviour of the battery charging pattern into account by using real measured EV charging data together with the consideration of an actual distribution system belonging to a region in Turkey. Lastly, a bunch of case studies is conducted in order to validate the accuracy and effectiveness of the devised model.

1 | INTRODUCTION

Electric vehicles (EV) have gained increasing interest as an alternative to conventional fossil fuel-powered transportation vehicles, particularly at the last decade mainly due to the financial and non-financial incentives provided by governments and utilities, and to their potential of curtailing greenhouse gas emissions. The number of EVs on the roads in 2018 has reached 5.1 million worldwide, accounting for 1.8% of the global vehicle sales [1]. However, widespread public acceptance of EVs is restricted by some factors and among them, two challenges, namely, unavailability or limited availability of EV charging stations (EVCSs) in especially rural areas and the long waiting times in EVCSs caused by their insufficient charging capacity and limited charging rate of charging units have substantial impacts [2].

In order to address the first problem mentioned above, the researchers have concentrated on the sizing and siting of EVCSs by considering various factors such as the relevant costs and charging demands. As for the latter, the use of faster charging technologies which have been enabled by the recent developments in batteries and power electronic equipment has come into prominence, particularly in the last years. These fast charging stations (FCSs) have the capability of fully charging a depleted EV battery in a period of less than 30 min while the time required to fully charge an EV using a slow charging unit is in a range between 3 and 17 h depending on the EV specifications [3, 4]. Therefore, a significant portion of the efforts in the literature of EVCS has been devoted to the optimal allocation of EVCS including fast charging technologies.

Among these efforts, aiming at reducing the investment and operational costs, a stochastic approach for the optimal construction and reinforcement of EVCSs was proposed in ref. [5], in which EV charging demand is determined by considering the historical charging demand and driving patterns. With the same objective, Davidov and Pantos [6] presented an optimization model for the layout of EVCSs and examined the effects of using a fast charging technology on the costs and charging times of EVs. Still for minimizing the costs, a mixed-integer linear programming (MILP) model and a second-order cone programming model were introduced in refs. [7] and [8], respectively, for EVCS planning with consideration of the constraints for both transportation and power networks. Besides, Zhou et al. [9] established a bi-level approach for the planning of FCSs by considering charging demands, where a flow refueling location method was employed in the upper level to reduce the planning costs and a traffic assignment method was used in the lower level to select the spatio-temporal distribution of EV flows over the network. Several authors have also adopted different objectives in their studies together with cost minimization. Kong et al. [10] developed a location planning approach for FCSs with the objective of optimizing various metrics such as traffic efficiency, the economy of operators and power loss of EVs in addition to total construction and operational costs. In order to determine the number and locations of EVCSs through their spatial distribution, Dong et al. [11] implemented a method based on a shared nearest neighbor clustering algorithm, which aims to minimize the sum of the charger and waiting costs. Mixed-integer non-linear programming (MINLP) problem was employed for optimal placing and sizing of EVCSs, which minimizes charging loss, together with station development and electrification costs [12].

Apart from the objective of minimizing the EVCS costs such as investment and operational costs, various single- or multi-objective functions have been also considered in the literature of EVCS planning. For instance, using an objective function of increasing EV demand, a flow refueling location problem was used in ref. [13] to select the locations and numbers of EV fast charging modules. For the same target, Wang et al. [14] examined the siting and sizing problem of FCSs in a highway network, and Wu and Sioshansi [15] developed an approach based on a flow capturing location model for optimizing the location of FCSs. Similarly, in order to meet the charging demands, Zhang et al. [16] developed a combined approach for sizing and siting of FCSs by considering the outputs of an agent-based simulation method, called BEAM, which describes the behaviours of transportation systems and passengers in cities, and produces mobility estimations. Besides, considering different objectives, an optimal planning solution for FCSs based on the formulation of EV fast charging demand was presented in ref. [17] for maximizing the expected CS profit, a planning model of FCSs based on Nash bargaining theory was presented in ref. [18] for determining their optimum size and site as well as optimizing the price of energy transacted between utility and EVCS, and long-distance travel data was used in ref. [3] to allocate EVCSs for increasing long-distance trip completions. The use of fast charging technologies in EVCSs might be a vital necessity in the case that charging times are critical for EV users. For instance, due to the higher number of charging operations during 1 day, electric taxis need to charge in very short periods. In order to enable this task, Morro-Mello et al. [19] studied a decision-making methodology to identify the optimal locations for FCSs. In another study for EV taxis [20], a data-driven optimization problem was presented in order to allocate EVCSs in a city with the objective of reducing investment costs.

It is evident from the studies above that most of the recent existing researches have considered the FCSs in the sizing and siting optimization problem and neglected the other types of charging facilities. However, in order to implement a more realistic approach, multi-type charging types, which might serve various EV types, might be taken into account. Motivated by this fact, Mehrjerdia and Hemmati [21] presented an approach for optimizing the sizing and siting of the EVCSs including slow, medium, and fast speed charging facilities with the objective of minimizing the investment and operational costs. For the purpose of minimizing energy losses, optimal sizing of CSs which have chargers with various charging levels and have the capability of providing reactive power support for EVs was investigated in ref. [22]. With the objective of determining the location of three types of charging units, a spatio-temporal flow capturing location model was proposed in ref. [4]. In order to mitigate the amount of over discharge rate of EVs, a mathematical layout optimization model for charging infrastructure was presented in ref. [23] by examining the proportions of slow and fast charging points.

In a few studies, multi-objective optimization problems were put forward for the EVCSs with different charging facilities. An EVCS allocation optimization model was developed in ref. [24] for minimizing the costs of investment, reinforcement, operation, and network loss of EVCSs comprising multi-types of charging facilities. Graber et al. [25] proposed a model to determine the type and number of EVCSs with different types of charging modes in a parking area while balancing the tradeoff between energy cost minimization and quality of service for users. A novel concept simultaneously optimizing the allocation of EVCSs with different charger levels, renewable generation units, and energy storage systems was developed in ref. [26] for

TABLE 1 Taxonomy of the study compared to the research in the literature

		EVCS						
References	**Objective**	**FCS**	**CS**	**Siting and Sizing**	**Power Losses**	**Battery Energy Management**	**Real Distribution Network**	**Uncertainties**
[5]	Min. The investment and operational cost	✓	✓	✓	✓	-	-	✓
[6]	Min. The investment and operational cost	✓	✓	✓	-	-	-	✓
[7, 8]	Min. The investment and operational cost	✓	-	✓	✓	-	-	✓
[9]	Min. The investment and operational cost	✓	-	✓	✓	-	-	✓
[10]	Min. The investment and operational cost	✓	-	✓	✓	-	✓	-
[11]	Min. The sum of chargers and waiting cost	✓	-	✓	-	-	-	✓
[12]	Min. The total cost	✓	-	✓	✓	-	✓	-
[13]	Max. The EV demand and flow coverage	✓	-	✓	-	-	-	-
[14]	Max. The overall EV flow	✓	-	✓	-	-	-	-
[15]	Max. The prospective EVs	✓	-	✓	-	-	-	✓
[16]	Min. The total cost	✓	-	✓	-	-	-	-
[17]	Max. The expected CS profit	✓	-	✓	-	-	-	✓
[18]	Max. The expected CS and distribution system operator profit	✓	-	✓	✓	-	-	-
[19]	Sustainable planning	✓	-	✓	-	-	-	✓
[20]	Min. The investment cost	✓	✓	✓	-	-	-	-
[21]	Min. The investment and operational cost	✓	✓	✓	-	-	-	✓
[22]	Min. The energy losses	✓	✓	✓	✓	-	-	-
[23]	Min. The total discharge	✓	✓	-	-	-	-	-
[24]	Min. The investment and operational cost and losses	✓	✓	✓	✓	-	✓	✓
[25]	Min. The total cost	✓	✓	✓	-	✓	-	✓
[26]	Min. The total loss and Max. The CS penetration	✓	✓	✓	✓	-	✓	-
[27]	Min. The investment cost and energy losses	✓	✓	✓	✓	-	-	✓
[28]	Min. The investment and operational cost, losses, emissions and traffic costs	✓	-	✓	✓	-	✓	✓
This study	Min. The total number of CSs	✓	✓	✓	✓	✓	✓	✓

either loss minimization or penetration maximization of EVCSs, renewable units, and storage systems. Another multi-objective planning model was introduced in ref. [27] for EVCSs with different types of charging stations in order to minimize the investment cost and energy loss of the distribution system and to maximize the annually captured traffic flow. Luo et al. [28] proposed a joint optimization method for minimizing investment and operational costs, as well as emissions, line losses, and traffic costs, without taking into account different types of CSs. The studies referred to above clearly show the increasing interest in the optimal EVCS planning problem including multi-type charging facilities. Besides, the importance of considering different types of charging facilities in CSs has been highlighted in other studies such as refs. [29–31], where slow charging stations were used and the use of FCSs was planned as a future study. Furthermore, a taxonomy is created in Table 1 to reflect the contributions of this work by considering the studies in the literature in a comparable manner. It can be deduced from the mentioned table that the study has some superiorities to the literature such as using real distribution system data and taking the uncertain behaviour of EVs into account together with the impact of battery energy management.

Here, therefore, the optimal sizing and siting problem of EVCSs with multi-type charging facilities in a distribution network is addressed. An MILP model for the mentioned problem is provided while evaluating the effectiveness of the proposed approach by different case studies.

The contributions of the study can be given as follows:

- The sizing and siting of EV charging stations with different charging rate levels are provided by an optimization framework in a real distribution system in which an active demand-side management capability can also be enabled.
- The proposed optimization model is also reformulated by modifying the objective function so that the siting and sizing of the EVCSs' number are minimized for a given demand, which has, to the best of our knowledge, not been investigated before.
- The real measured data are used for EV power demand, by doing so the battery energy management system of the EVs

has been modelled and the case studies are performed in a real distribution system to obtain more realistic results. In addition, the historic data are considered in order to address the EV-related uncertainties.

Table 1 summarizes the contribution of this study to the existing literature.

The remainder of the paper is organized as follows: the proposed optimization model is presented in Section 2. Then, the effectiveness of the proposed methodology is examined through a representative test case with relevant discussions in Section 3. Finally, concluding remarks and directions for future studies are presented in Section 4.

2 | SYSTEM DESCRIPTION AND METHODOLOGY

A MILP-based model is propounded for the optimal sizing and siting of different CS types in a distribution system in this study. Furthermore, the proposed model takes into consideration the power flow among the buses with the aid of linear approximation of the losses on the branches.

2.1 | Objective function

The main objective of the devised model is to minimize the total number of CSs in the system for the fulfilment of the charging necessity of EVs, as stated in (1).

$$\min TCSC = \sum_i \sum_n \sum_j u_{i,n,j} * P_n^{CS-cap} \tag{1}$$

Where the number of each type of CSs in different nodes is calculated using (2).

$$N_{i,n}^{CS} = \sum_j u_{i,n,j} \tag{2}$$

2.2 | The distribution system constraints

Equation (3) describes the overall power balance of the system for each period for each node. The term $P_{i,t}^{\text{load\_other}}$ represents the other loads fed at the related node for the period t. The total power consumption of EVs connected to each node for the period t is expressed by $P_{i,t}^{\text{EV\_dem\_tot}}$. The summation of both quantities has to be equal to the power flowing to the related node on the branches during the period t. It is worthy to underline that the power flow in this model is assumed as from upstream grid to the loads in a single direction as distributed generation (DG) availability is not considered in this study. Besides, the power transmission capacity of each branch is determined by (4). Also, the power balance for the upstream node is described in (5). In this equation, $P_{i,t}$ indicates the power limit of the generator located at node i. Hence, the power demands of the other loads and EVs along with the power losses on branches can be met from the upstream grid. Moreover, the power limit of generator needs to be determined as in (6).

$$P_{i,t}^{f,\text{ load}} + \sum_{b\in B:i\in\Omega_l^j} f_{b,t} - \sum_{b\in B:i\in\Omega_l^i} f_{b,t} = P_{i,t}^{\text{EV\_dem\_tot}} + P_{i,t}^{\text{load\_other}} \quad \forall i \in I, \forall t \in T \tag{3}$$

$$0 \le f_{b,t} \le f_b^{\max}, \quad \forall b \in B, t \in T \tag{4}$$

$$P_{i,t} = P_{i,t}^{f,\text{load}} + \sum_{b\in B} P_{b,t}^{\text{loss}}, \quad \forall i \in \Omega_i^f, t \in T \tag{5}$$

$$0 \le P_{i,t} \le P_i^{\max}, \quad \forall i \in \Omega_i^f, t \in T \tag{6}$$

2.3 | Linear approximation of the losses

Equation (7) expresses the total power losses on a related branch, consisting of a second-order function with d and c constants. However, this expression has a non-linear term $(f_{b,t}{}^2)$ that has to be linearized. To serve this purpose, a well-known linearization method, named Special Order Sets of Type 2 (SOS2), is included so as to obtain convenient approximation into the MILP framework. Equation (8) indicates the SOS2 variables during the approximation of power flow on the branches with the constraints given in (9) and (10).

$$P_{b,t}^{\text{loss}} = d * |f_{b,t}| + c * f_{b,t}{}^2, \quad \forall b \in B, \forall t \in T \tag{7}$$

$$\sum_{p\in P} z_{b,t,p} = 1, \quad \forall b \in B, \forall t \in T \tag{8}$$

$$f_{b,t} = \sum_{p\in P} X_p * z_{b,t,p}, \quad \forall b\, inB, \forall t \in T \tag{9}$$

$$F_{b,t} = \sum_{p\in P} Y_p * z_{b,t,p}, \quad \forall b\, inB, \forall t \in T \tag{10}$$

2.4 | EV charging limitations and battery constraints

The total power demand of EVs in node i during period t is equal to the summation of the power demand of each EV charging from the CS located in the related node, as stated in (11). The power consumption of an EV cannot exceed the charging limit of the mentioned EV imposed by (12) based on activation of different phases regarding charging power levels of a CS type based on EV state-of-energy (SoE) due to the phase transitions considering (13) and (14). Equation (15) describes the SoE changes of the related EV during the charging period, in which $SoE_{i,k,t-1}^{\text{EV}}$ represents the previous SoE level of the EV and $P_{i,k,t}^{\text{EV}} * CE_k^{\text{EV}} * \Delta T$ stands for the charging energy during period t. Furthermore, Equations (16)–(18) determine the initial SoE level of the EV when it is plugged in, the desired SoE level

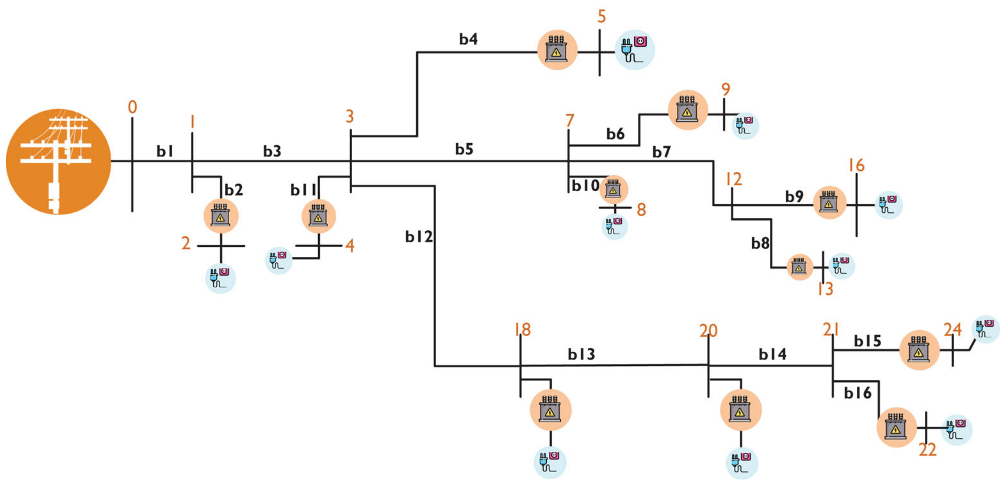

FIGURE 1 Single line diagram of the evaluated distribution system

of the EV at the departure period, and the boundaries for the SoE of the EV battery, respectively. Finally, the SoE and the charging power values of each EV must not take any value in the periods when it is not plugged in any CS, as provided in (19).

$$P_{i,t}^{\text{EV\_dem\_tot}} = \sum_{k} P_{i,k,t}^{\text{EV}}, \quad \forall i, \forall T \tag{11}$$

$$\sum_{k} P_{i,k,t}^{\text{EV}} \leq P_{i,k,t}^{\text{EV-ch-lim}}, \forall i, \forall k, \forall t \in [T_{i,k}^{a}, T_{i,k}^{d}] \tag{12}$$

$$P_{i,k,t}^{\text{EV-ch-lim}} = \sum_{p} \sum_{n} P_{n,p}^{\text{ch-lim}} * y_{i,k,n,p,t}^{ph}, \quad \forall i, \forall k, \forall t \in [T_{i,k}^{a}, T_{i,k}^{d}] \tag{13}$$

$$\sum_{p} \sum_{n} SoE_{k,p}^{\text{EV-lim}} * y_{i,k,n,p,t}^{ph}, \quad \forall i, \forall k, \forall t \in [T_{i,k}^{a}, T_{i,k}^{d}] \tag{14}$$

$$SoE_{i,k,t}^{\text{EV}} = SoE_{i,k,t-1}^{\text{EV}} + P_{i,k,t}^{\text{EV}} * CE_{k}^{\text{EV}} * \Delta T, \quad \forall i, \forall k, \forall t \in [T_{i,k}^{a}, T_{i,k}^{d}] \tag{15}$$

$$SoE_{i,k,t}^{\text{EV}} = SoE_{i,k}^{\text{EV,ini}}, \quad \forall i, \forall k, t = T_{i,k}^{a} \tag{16}$$

$$SoE_{i,k,t}^{\text{EV}} = SoE_{i,k}^{\text{EV,des}}, \quad \forall i, \forall k, t = T_{i,k}^{d} \tag{17}$$

$$SoE_{i,k}^{\text{EV,min}} \leq SoE_{i,k,t}^{\text{EV}} \leq SoE_{i,k}^{\text{EV,max}}, \forall i, \forall k, \forall t \tag{18}$$

$$SoE_{i,k,t}^{\text{EV}} = 0, P_{i,k,t}^{\text{EV}} = 0, \forall i, \forall k, \forall t \notin [T_{i,k}^{a}, T_{i,k}^{d}] \tag{19}$$

2.5 | Additional logical constraints

In order to perform the charging transactions of each EV properly with the purpose of minimizing the number of CS to be

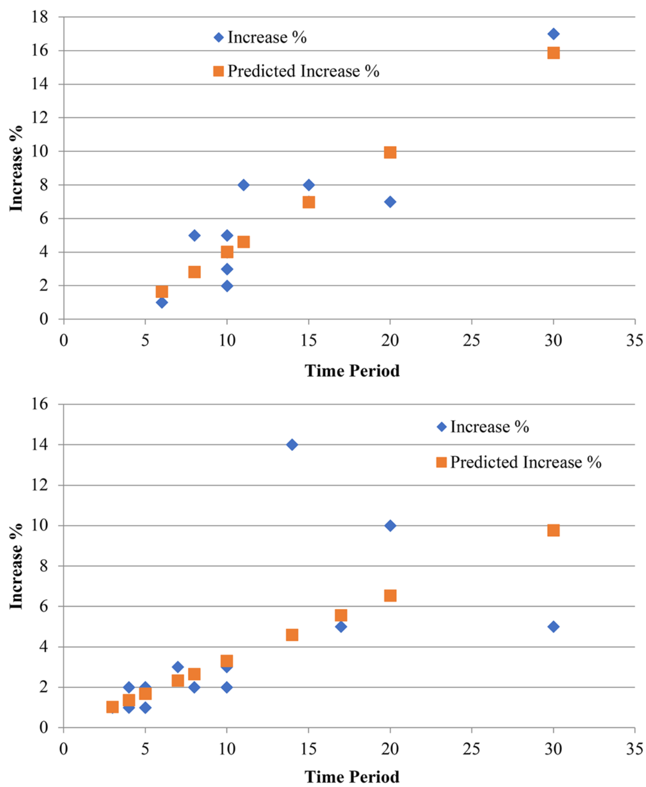

FIGURE 2 Comparison of state of charge realized percentage increase and estimated percentage increase rate for ZoE-1 and ZoE-2 vehicles

located in the system, some additional logical constraints are implemented into the devised model.

A CS of type n can be located into a single node thanks to the binary variable stated in (20). Equation (21) prevents the total number of EVs in charging state by a CS type within each period t to exceed the number of the mentioned type of CS in the related node. Constraint (22) determines the matching of EVs to a CS type. Herein, if an EV starts to charge, there cannot be any new EV to be plugged in at the same CS until the

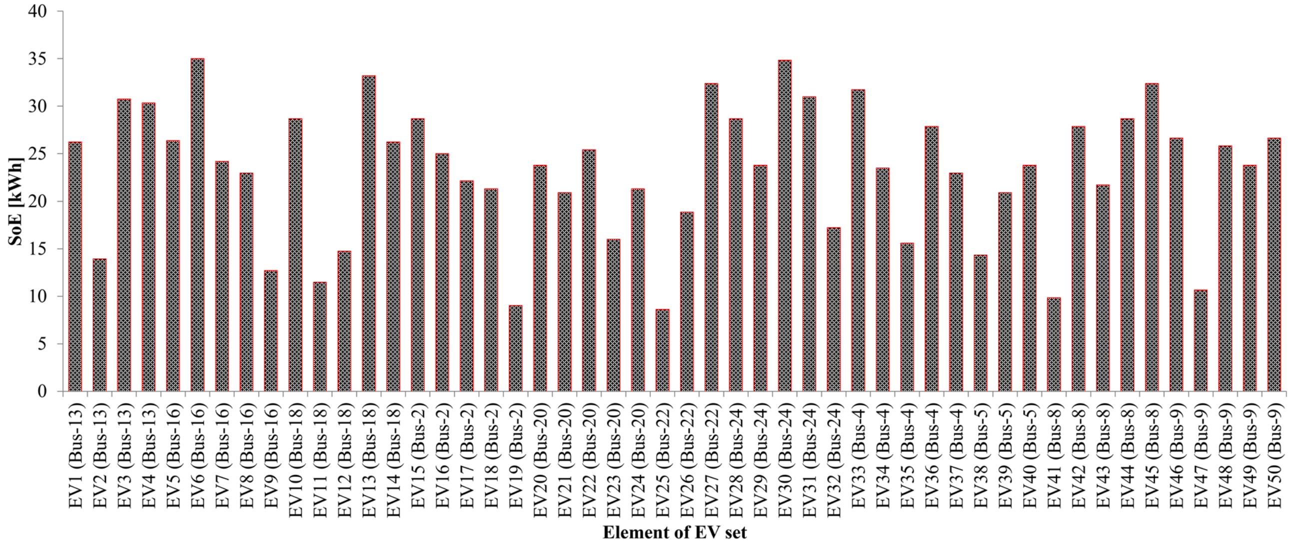

FIGURE 3 The initial state-of-energy values of the considered electric vehicles

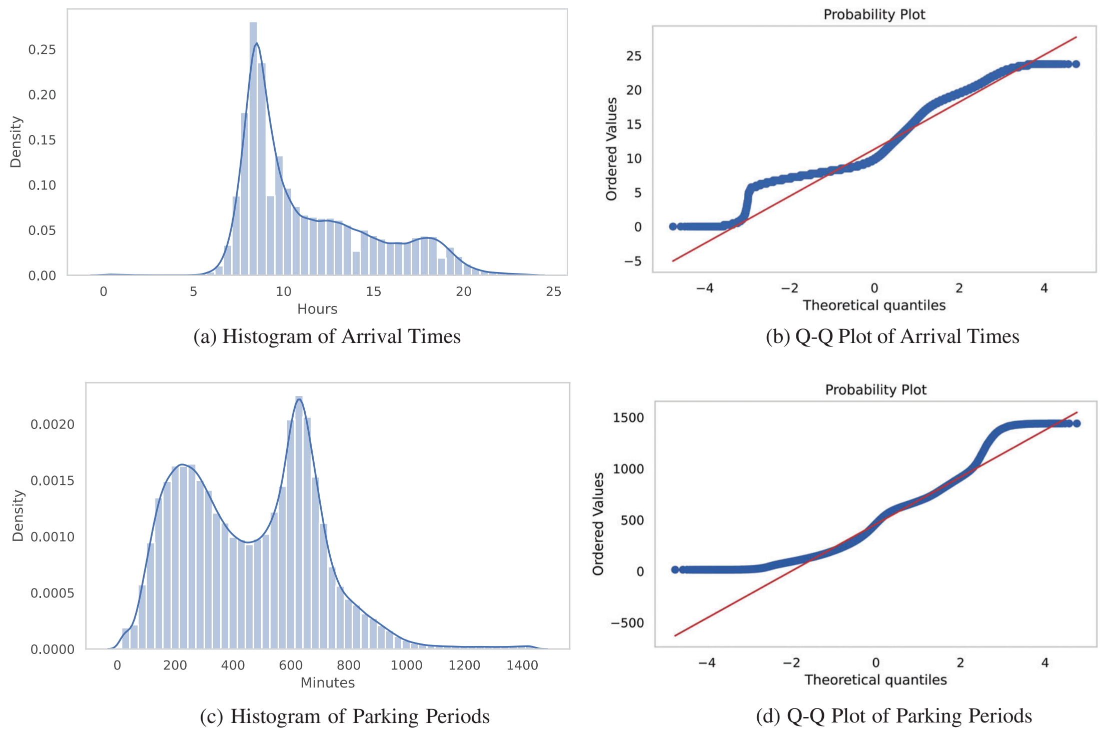

FIGURE 4 Statistics for 4-year real data of a parking lot. (a) Histogram of Arrival Times, (b) Q-Q Plot of Arrival Times, (c) Histogram of Parking Periods, and (d) Q-Q Plot of Parking Periods

current EV reaches to the desired SoE level regarding the constraints in (23)–(26). Different charging phases cannot be active simultaneously or cannot be activated if the mentioned EV is not in charging status based on (27). The dynamics of different phases of charging status are modelled using (27)–(31) while the consecutive transition between them to enable the mimicry of the realistic relationship between SoE of EV and maximum power limit of a CS is considered using (32) where the end of the active status of a charging phase automatically initiates the activation of the following phase.

$$\sum_{i} u_{i,n,j} \leq 1, \quad \forall n, \forall j \tag{20}$$

$$\sum_{k} y_{i,k,n,t} \leq \sum_{j} u_{i,n,j}, \quad \forall i, \forall n, \forall t \tag{21}$$

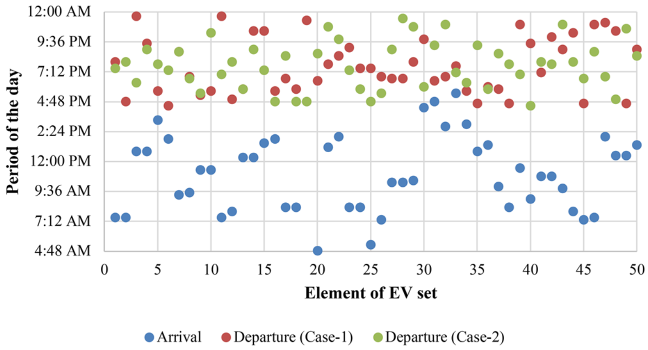

FIGURE 5 The arrival and departure times of the considered electric vehicles

$$\sum_{n} y_{i,k,n,t} \leq 1, \quad \forall i, \forall k, \forall t \in [T^{a}_{i,k}, T^{d}_{i,k}] \tag{22}$$

$$y_{i,k,n,t} - y_{i,k,n,t-1} = x_{i,k,n,t} - z_{i,k,n,t}, \quad \forall i, \forall k, \forall n, \forall t \in [T^{a}_{i,k}, T^{d}_{i,k}] \tag{23}$$

$$x_{i,k,n,t} + z_{i,k,n,t} \leq 1, \forall i, \forall k, \forall n, \forall t \in [T^{a}_{i,k}, T^{d}_{i,k}] \tag{24}$$

$$\sum_{n} \sum_{t} x_{i,k,n,t} = 1, \quad \forall i, \forall k \tag{25}$$

$$\sum_{n} \sum_{t} z_{i,k,n,t} = 1, \quad \forall i, \forall k \tag{26}$$

$$\sum_{p} y^{ph}_{i,k,n,p,t} = y_{i,k,n,t}, \forall i, \forall k, \forall n, \forall t \in [T^{a}_{i,k}, T^{d}_{i,k}] \tag{27}$$

$$y^{ph}_{i,k,n,p,t} - y^{ph}_{i,k,n,p,t-1} = x^{ph}_{i,k,n,p,t} - z^{ph}_{i,k,n,p,t}, \quad \forall i, \forall k, \forall n, \forall p, \forall t \in [T^{a}_{i,k}, T^{d}_{i,k}] \tag{28}$$

$$x^{ph}_{i,k,n,p,t} + z^{ph}_{i,k,n,p,t} \leq 1, \quad \forall i, \forall k, \forall n, \forall p, \forall t \in [T^{a}_{i,k}, T^{d}_{i,k}] \tag{29}$$

$$\sum_{t} x^{ph}_{i,k,n,p,t} = 1, \forall i, \forall k, \forall n, \forall p \tag{30}$$

$$\sum_{t} z^{ph}_{i,k,n,p,t} = 1, \forall i, \forall k, \forall n, \forall p \tag{31}$$

$$z^{ph}_{i,k,n,p,t} = x^{ph}_{i,k,n,p+1,t}, \quad \forall i, \forall k, \forall n, \forall p < card(p), \forall t \in [T^{a}_{i,k}, T^{d}_{i,k}] \tag{32}$$

3 | TEST AND RESULTS

3.1 | Input data

The proposed optimization model has been tested with the Bozuyuk region, which is a part of the Turkey distribution system managed by Osmangazi Elektrik Dagitim A.S. (OEDAS). Figure 1 shows the single line diagram of Bozuyuk distribution region with the demonstrations of substations and CSs. In addition, the other loads fed by the transformers in the related region are also considered throughout the simulations. Besides, state-of-charge (SoC) patterns based on the actual measurements performed during two different charging processes of the Renault ZOE, one of Renault's EV brands, are provided. During the testing of the devised model, the charging process is realized by using these patterns to obtain a more realistic SoE (SoC values are converted to the SoE values and hereafter referred to as SoE) change. Hence, the actual dynamics of the EV battery charging process are provided as an input to the model. Regression analysis for Renault ZOE-1 and ZOE-2 vehicles has been performed; the level of significance for both measurements has been obtained as quite lower than 5%, almost equals to zero. Figure 2 demonstrates the comparison of SoC realized and estimated percentage increase for ZOE-1 and ZOE-2, respectively. By doing so, the battery energy management system for the Renault ZOE vehicle is modelled to obtain more realistic charging pattern. The charging rates for ZOE are determined as 22 kW up to 80% (33 kWh), 11 kW between 80% and 95% (33–39 kWh), and 1.2 kW after 95% (39 kWh). A group of EVs includes 50 Renault ZOE models, which have different initial SoE levels just before plug-in along with various arrival times that are considered during the simulations. The initial SoE levels and distributed bus names are given in Figure 3.

Four years of data consisting of 715,651 vehicles from a parking lot in Istanbul, Turkey, is utilized to estimate the arrival and departure times of EVs. The histogram and quantile–quantile (Q–Q) graphics of the arrival times and parking times of the vehicles are shown in Figure 4. It can be seen that the pattern of the dataset used is similar to that of a normal distribution. Thus, a random normal distribution can be used to generate synthetic EV parking data. The arrival and departure times of the 50 EVs utilized in this study are calculated using these statistics from 4 years of real data using Python SciPy library.

3.2 | Simulation and results

The model has been coded in GAMS 24.0.2 and solved by the commercial solver CPLEX 12 on a computer with a 2.3 GHz CPU and 32 GB of RAM. To investigate the effectiveness of the devised model, three different case studies have been created as follows: departure times of EVs are generated using yearly statistics in Case 1 and Case 2. It is assumed that EVs should lastly leave the charging stations at 7 PM, 9 PM, and 12 AM in Case 3, Case 4, and Case 5, respectively, to analyze the effect of long parking periods. Arrival and departure times of EVs are depicted in Figure 5. Also, it should be noted that Cases 3, 4, and 5 are not presented in this graph for convenience of analysis. Two types of CSs are considered, namely Type I and Type II, with capacities of 7.2 and 22 kW, respectively.

Table 2 encapsulates the final results for each case study and provides a comprehensive comparison among them. It can be seen in Table 2 that the greatest number of CS is located in Cases 3–5 due to the fact that all EVs have the same

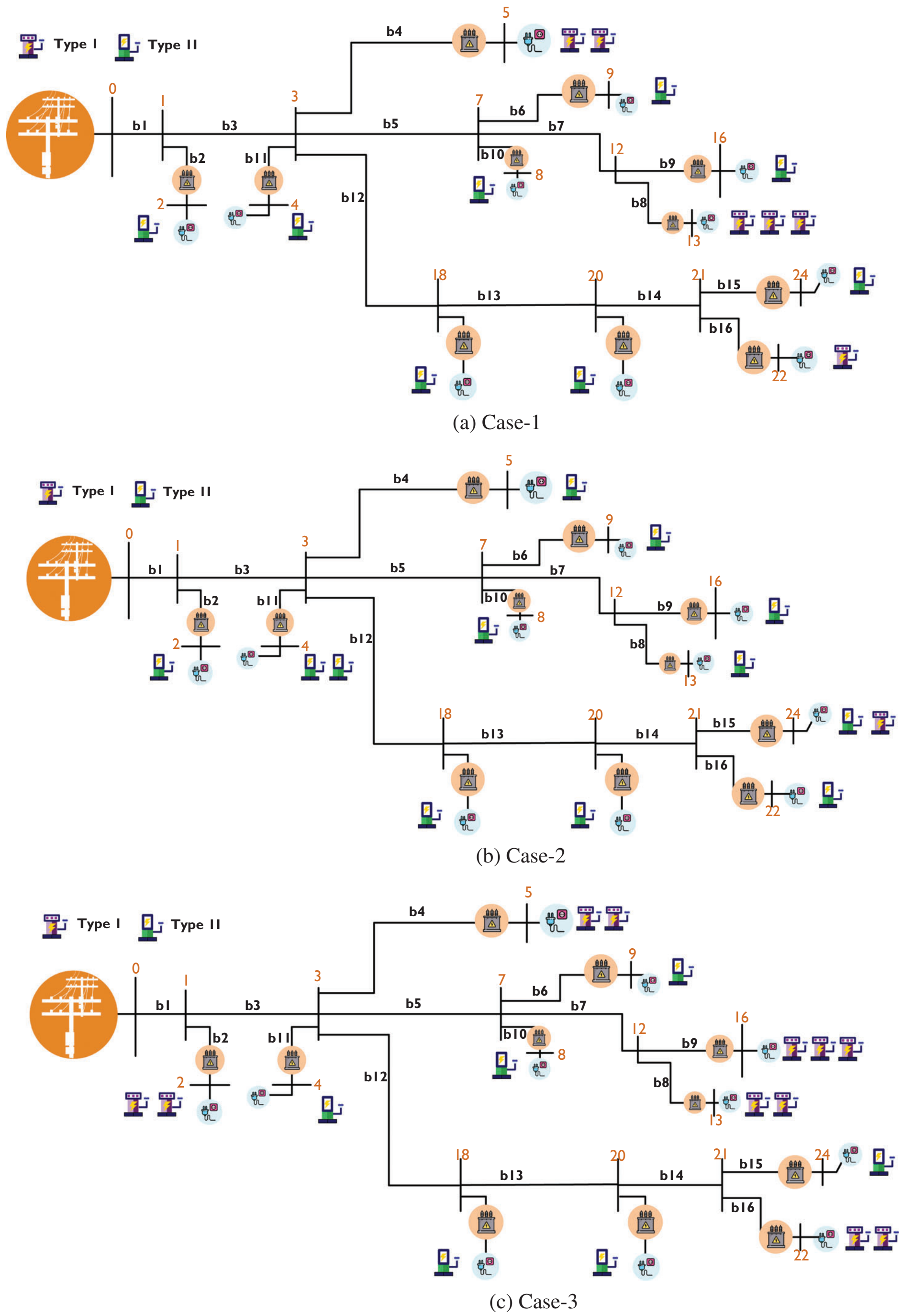

FIGURE 6 Demonstration of the located charging stations in the evaluated distribution system for (a) Case 1, (b) Case 2, and (c) Case 3

departure time. However, because of the long parking times, Case 5 has the least Type-II chargers. The charging demand is met using Type-I chargers rather than Type-II chargers when the amount of parking time increases. Consequently, there are far fewer Type-II chargers in the system. In Case 5, only one Type-II charger is needed. Moreover, it can be concluded that as the main aim of the model, the number of total CSs is minimized in each bus thanks to the different arrival times of related EVs. Furthermore, the departure time limitations have also impact on clarifying the total number of CSs. The detailed demonstration of located CS types on the considered distribution system for each case study is shown in Figure 6.

Figure 7 shows the power consumption of Bus 8, Bus 9, Bus 18, and Bus 20, which same number of CS types are located in to charge the plugged EVs. The power consumption for different cases is different due to the departure time of EVs, as seen in each subfigure. Moreover, five EVs have reached Bus 8, Bus 9, Bus 18, and Bus 20 for charging operations. Due to the arrival

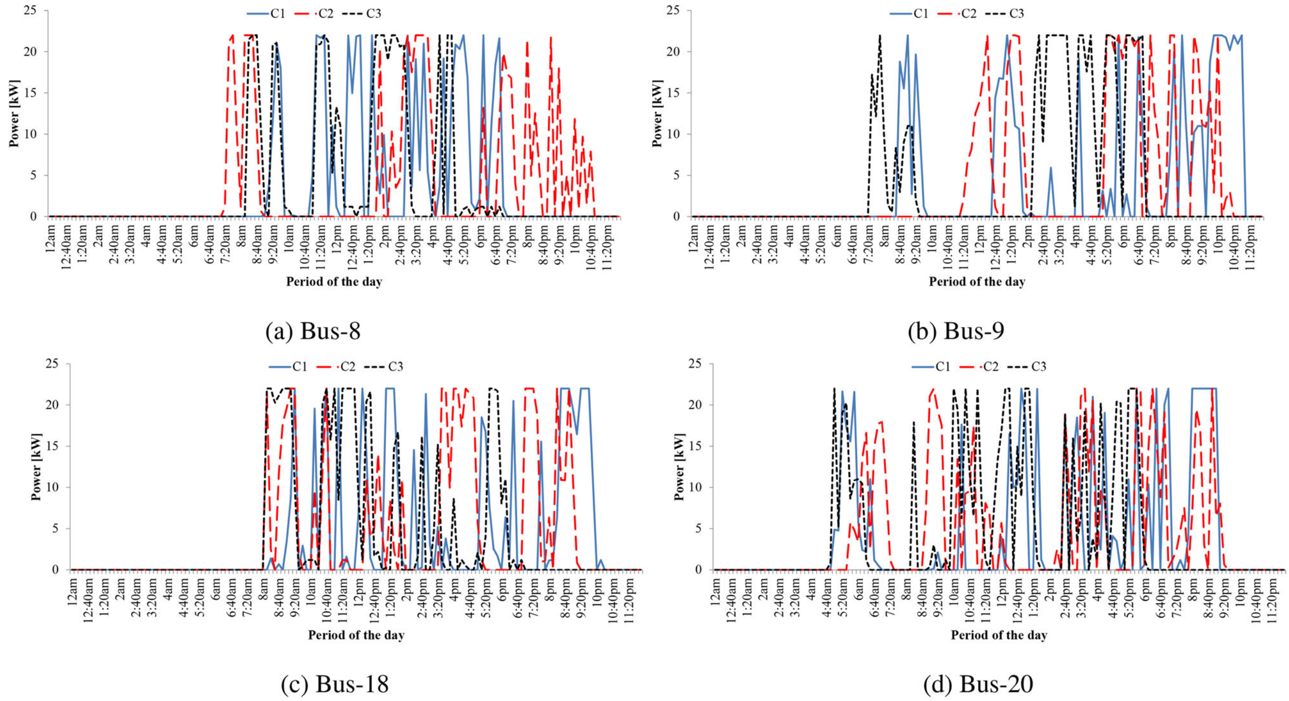

FIGURE 7 The results of the buses without changes in number and type of charging stations among Case 1, Case 2, and Case 3. (a) Bus-8, (b) Bus-9, (c) Bus-18, and (d) Bus-20

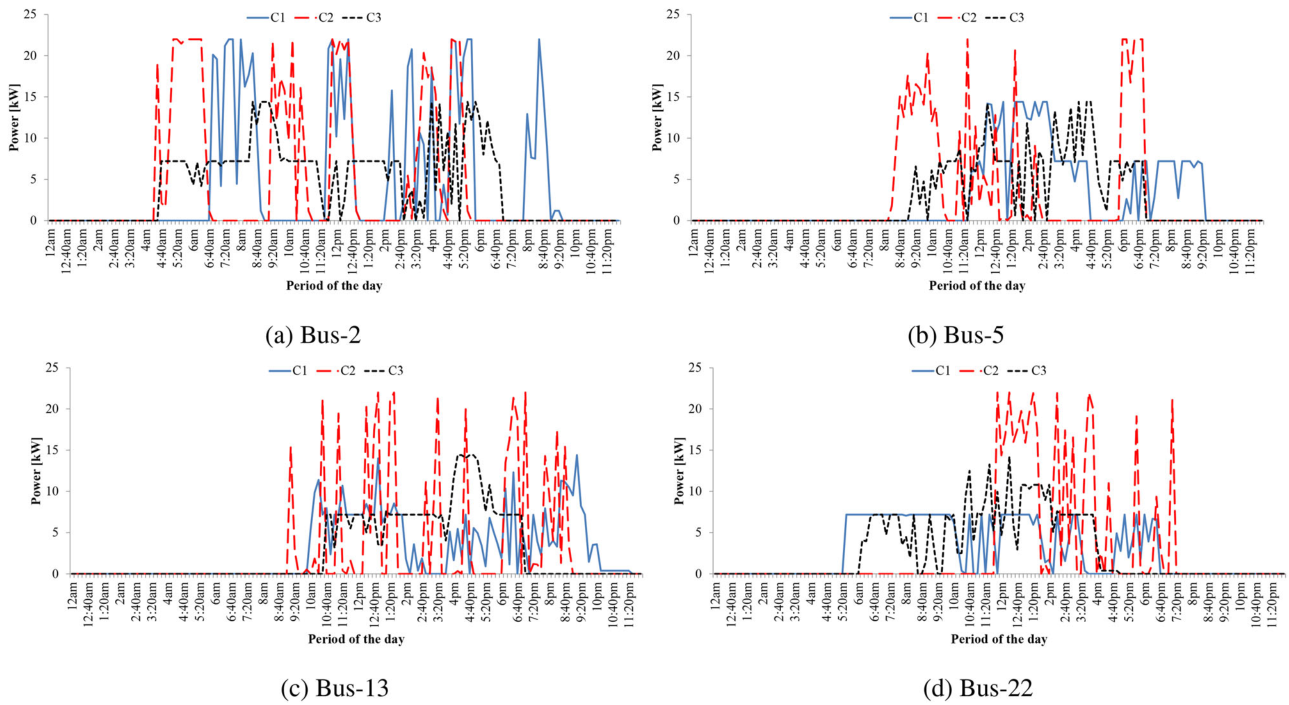

FIGURE 8 The results of the buses with changes in number and type of charging stations among Case 1, Case 2, and Case 3 . (a) Bus-2, (b) Bus-5, (c) Bus-13, and (d) Bus-22

times of EVs, the proposed model has sited one Type-II CS in each bus for all cases. However, it is obviously seen that Case 3 has fewer power peaks for all buses since Case 3 has longer parking periods than Case 1 and Case 2.

Figure 8 presents the power drawn from the Bus 2, Bus 5, Bus 13, and Bus 22 for Case 1, Case 2, and Case 3. It is needed to highlight that there are five, three, four, and three EVs for charging operation at Bus 2, Bus 5, Bus 13, and Bus 22, respectively.

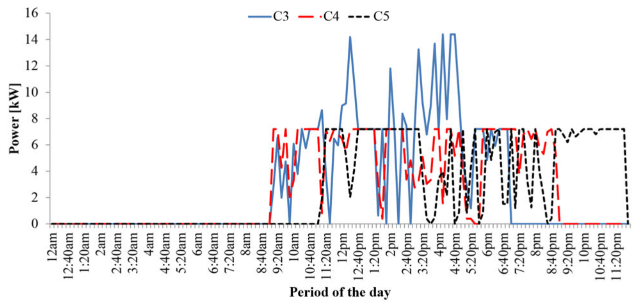

(a) Bus-5

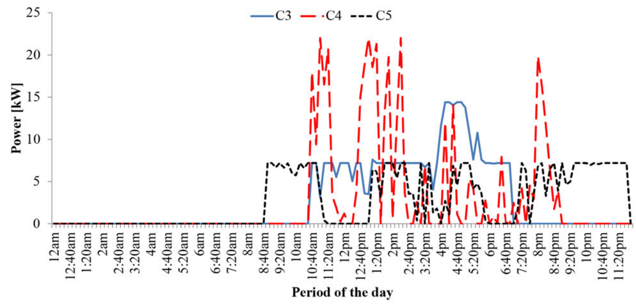

(b) Bus-13

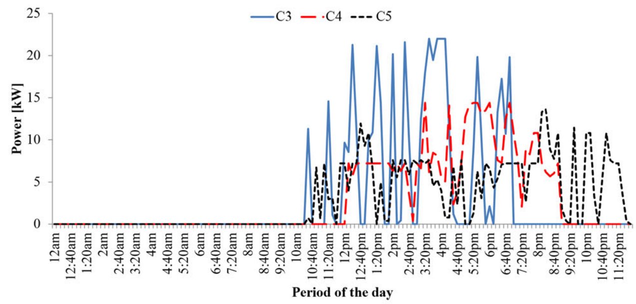

(c) Bus-24

FIGURE 9 The results of the Case 3, Case 4, and Case 5 with different departure times for (a) Bus-5, (b) Bus-13, and (c) Bus-24

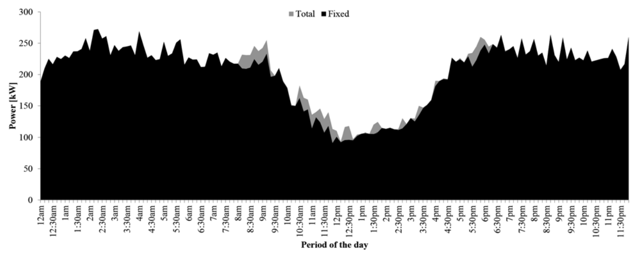

FIGURE 10 The change of power consumption in Bus 18 after electric vehicles included for Case 3

Since less number of EVs are charged at Bus 5, Bus 13, and Bus 22, the power consumption of the related buses is not remarkably as much as that of Bus 2. Another reason for that reduction is the arrival times of EVs, because the model can minimize the total number of CSs owing to the more flexible time periods. In addition, the power demand curve has few peaks in Case 3 compared to the other cases because of the more flexible parking period. By further detailed examination in Figure 8d, it can be observed that even there are three EVs at Bus 22; while one and two Type-I chargers are enough to fully charge the EVs in

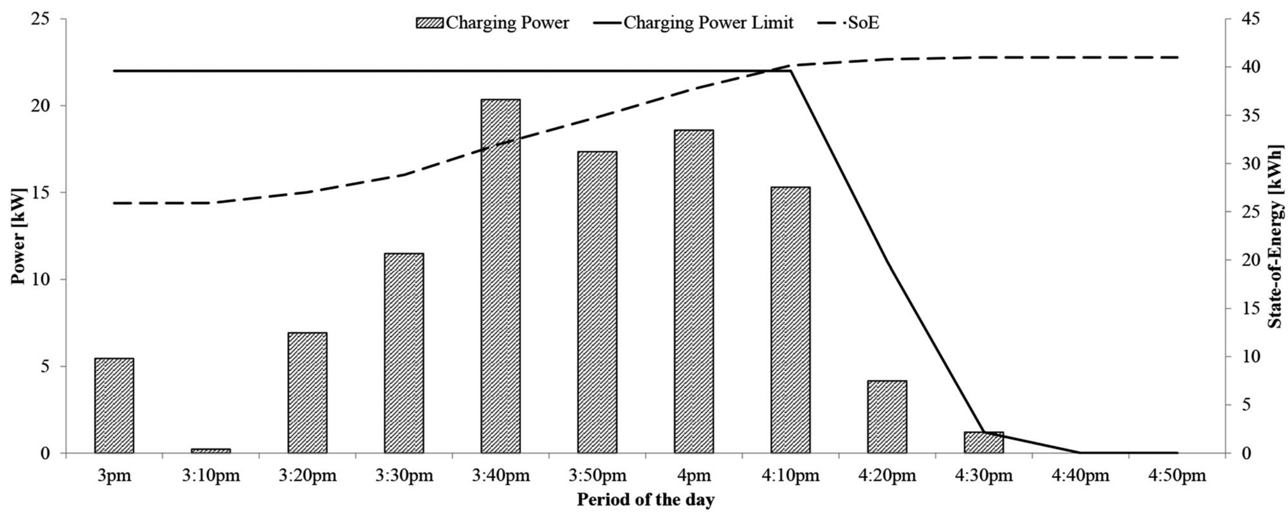

FIGURE 11 The state-of-energy variation of EV16 with respect to charging power

TABLE 2 The results for located number of different charging station types

		Case 1		Case 2		Case 3		Case 4		Case 5	
Bus	**No. of EVs**	**Type I**	**Type II**	**Type I**	**Type II**	**Type I**	**Type II**	**Type I**	**Type II**	**Type I**	**Type II**
Bus 2	5	0	1	0	1	2	0	2	0	4	0
Bus 4	5	0	1	0	2	0	1	2	0	2	0
Bus 5	3	2	0	0	1	2	0	1	0	1	0
Bus 8	5	0	1	0	1	0	1	2	0	1	0
Bus 9	5	0	1	0	1	0	1	2	0	1	1
Bus 13	4	3	0	0	1	2	0	0	1	1	0
Bus 16	5	0	1	0	1	3	0	2	0	2	0
Bus 18	5	0	1	0	1	0	1	1	1	1	0
Bus 20	5	0	1	0	1	0	1	0	1	1	0
Bus 22	3	1	0	0	1	2	0	1	0	1	0
Bus 24	5	0	1	1	1	0	1	2	0	2	0
TOTAL	**50**	**6**	**8**	**1**	**12**	**11**	**6**	**15**	**3**	**17**	**1**

Case 1 and Case 3, respectively, one Type-II charger is sited in Case 2. Case 1 and Case 3, on the other hand, have more flattened power curves; however, using a Type-II charger produces more peaks than the other cases. In addition, in cases where fast charging is used, frequent power changes occur due to the battery management system model proposed in this study that manages the varying charging power at different SoC levels. As a result, power variations should be taken into account when designing a system.

Figure 9 illustrates how the length of the parking period affects the amount of power drawn from the grid in case studies 3–5. When the Bus 5 results are analyzed, it is clear that the peak power is reduced because Cases 4 and 5 do not require the Type-II charger that was required in Case 3. While the charging demand is satisfied by two Type-II CS in Case 3, the charging demand can be fulfilled by one Type-II charger in Case 4 in Bus 13, as shown in the Figure 9b. However, this results in new peak power. In Case 5, with the prolongation of the parking period, Type-II charger becomes unnecessary and one Type-I charger is sufficient to meet demand. In Case 3, one Type-II charger is used to meet the charging needs of EVs in Bus 24 as shown in Figure 9c, whereas in Cases 4 and 5, charging demand is fulfilled by two Type-I chargers without the requirement of a Type-II charger. Additionally, the peak power is decreased. Besides it is seen in Case 5 that the charging power is dispersed throughout the day due to the long parking period.

Figure 10 indicates the variation of the power consumption at Bus 18 after the penetration of EVs. While the black graph represents the fixed power demand of the related transformer, the grey one shows the total power curve by EVs' charging requests. Although there is only one Type-II charger at Bus 18, the power demand is noticeably increased after EVs introduction. It is solid proof that during the new installations related to CSs at any bus in the distribution system, the impact of charger type should be considered in terms of both economic and technical aspects. Figure 11 represents the relations between the charging power rate and the SoE level variation of EV16. It can be clearly seen in the graphs that the devised model can mimic the actual charging rate steps, which are modelled by using real measured charging patterns of two different Renault ZOE. The charging rate steps are a maximum of 22 kW charging rate up to 80% SoC (33 kWh), 11 kW between 80% and 95% (33–39 kWh), and 1.2 kW after 95% (39 kWh). Last but not least, the charging rates take value under those charging rate limits so as to perform active demand-side management which is obviously proven in that figure.

4 | CONCLUSIONS

This study investigates an optimization model that provides optimal sizing and siting of EVCSs in a distribution system. The main objective of the devised model is to minimize the total number of EVCSs to fulfill the EVs' charging demand by considering the network constraints along with the actual EV battery charging pattern. Real measured data pertaining to charging power patterns belonging to two different Renault ZOEs are utilized throughout the study. Also, the developed model is tested in a real distribution system, which is in a part of Turkey, managed by the OEDAS so as to show the validity of the model by considering three different case studies. The other measured loads fed by the related substations are also taken into consideration during the test of the model. Based on the findings, it is concluded that the proposed model is able to determine the optimal number of EVCSs based on different charging types. As well as enabling active demand-side management, the proposed model also provides an opportunity to charge EVs. It is worth underlining that the installation costs and additional renewal of the existing infrastructure might be prevented successfully owing to the devised model. However, this study does not examine the peak powers resulting from increased charging power and the possible effects of ancillary services that EVs can provide to the distribution system through different battery operation types such as vehicle-to-grid and vehicle-to-vehicle. In future study, this study would be improved by taken into account distribution system operator (DSO) and CS interactions.

ACKNOWLEDGEMENTS

This work was supported by the Energy Market Regulatory Authority of Turkey (EPDK) R&D Funds (project "The Investigation of the Effects of Electric Vehicles and Charging Stations on Power Grid and Development of Required National Software to Optimize These Loads") and The Scientific and Technological Research Council of Turkey (TUBITAK) under project Grant No. 119E215. The work of Ibrahim Şengör was supported by Science Foundation Ireland (SFI) under Grant No. 12/RC/2302_P2. Joao P. S. Catalão also acknowledges the support by FEDER funds through COMPETE 2020 and by Portuguese funds through FCT, under POCI-01-0145-FEDER-029803 (02/SAICT/2017).

CONFLICT OF INTEREST

The authors declare no conflict of interest.

DATA AVAILABILITY STATEMENT

Research data are not shared.

NOMENCLATURE

The abbreviations, sets and indices, parameters, and variables used throughout the study are stated below.

Abbreviations

CS	Charging station
DG	Distributed generation
DS	Distribution system
FCS	Fast charging station
EV	Electric vehicle
EVCS	Electric vehicle charging station
MILP	Mixed-integer linear programming
SoE	State-of-energy

Sets and Indices

b	Set of branches
i	Set of nodes
j	Set of CSs
k	Set of EVs
n	Set of CS types
t	Period of the day index in time units [min]

Parameters

ΔT	Time granularity
CE_k^{EV}	Charging efficiency of EV k [%]
f_b^{max}	Power transmission capacity of branch b [%]
N	Sufficiently large positive number
P_n^{CS-cap}	Capacity of CS type n [kW]
$P_{n,p}^{ch-lim}$	Charging power limit of phase p of CS type n [kW]
$P_i^{f,max}$	Power injection limit of upstream grid [kW]
$P_{i,t}^{load,ther}$	Power demand of other loads at node i for the period t [kW]
$SoE_{i,k}^{EV,des}$	Desired SoE of EV k in the region fed by node i at the departure time [kWh]
$SoE_{i,k}^{EV,ini}$	Initial SoE of EV k in the region fed by node i [kWh]
$SoE_{k,p}^{EV,lim}$	SoE limit of charging phase p of EV k [kWh]
$SoE_{i,k}^{EV,max}$	Maximum SoE of EV k in the region fed by node i [kWh]
$SoE_{i,k}^{EV,min}$	Minimum SoE of EV k in the region fed by node i [kWh]
$T_{i,k}^{a}$	Arrival time of EV k in the region fed by node i
$T_{i,k}^{d}$	Departure time of EV k in the region fed by node i
Y_p	Y-Coordinate of point p used in SOS2
X_p	X-Coordinate of point p used in SOS2

Decision Variables

$F_{b,t}$	Approximate value of the square of the power flow on branch b in period t [kW^2]
$f_{b,t}$	Active power flow on branch b in period t [kW]
$N_{i,n}^{CS}$	Number of CS j of type n in node i
$P_{i,t}$	Power drawn from the grid during period t [kW]
$P_{i,k,t}^{EV}$	Charging power of EV k in the region fed by node i during period t [kW]
$P_{i,k,t}^{EV-ch-lim}$	Charging power limit of EV k in the region fed by node i during period t [kW]
$P_{i,t}^{EV\_dem\_tot}$	The total power demand of EVs in node i during period t [kW]
$P_{b,t}^{loss}$	Power losses of branch b in period t [kW]
$SoE_{i,k,t}^{EV}$	SoE of EV k in the region fed by node i during period t [kWh]
$TCSC$	Total capacity of CSs located in the distribution system
$u_{i,n,j}$	The binary variable representing the availability of CS j of type n in node i: 1 if available, else 0
$x_{i,k,n,t}$	The binary variable representing the beginning of active status of charging status of EV k connected to CS j of type n in the region fed by node i during period t
$x_{i,k,n,p,t}^{ph}$	The binary variable representing the beginning of active status of charging phase p during period t for EV k connected to CS j of type n in the region fed by node i
$y_{i,k,n,t}$	The binary variable representing the active status of charging status of EV k connected to CS j of type n in the region fed by node i during period t
$y_{i,k,n,p,t}^{ph}$	The binary variable representing the active status of charging phase p during period t for EV k connected to CS j of type n in the region fed by node i
$z_{i,k,n,t}$	The binary variable representing the end of active status of charging status of EV k connected to

$z^{ph}_{i,k,n,p,t}$ — CS j of type n in the region fed by node i during period t

The binary variable representing the end of active status of charging phase p during period t for EV k connected to CS j of type n in the region fed by node i

ORCID

Ibrahim Sengor https://orcid.org/0000-0002-9451-4218

REFERENCES

1. International Energy Agency (IEA), Global ev outlook 2019, 232. (2019)
2. Philipsen, R., Schmidt, T., van Heek, J., Ziefle, M.: Fast-charging station here, please! User criteria for electric vehicle fast-charging locations. Transp. Res. F: Traffic Psychol. Behav. 40, 119–129 (2016)
3. He, Y., Kockelman, K.M., Perrine, K.A.: Optimal locations of U.S. fast charging stations for long-distance trip completion by battery electric vehicles. J. Cleaner Prod. 214, 452–461 (2019)
4. Abdalrahman, A., Zhuang, W.: PEV charging infrastructure siting based on spatial-temporal traffic flow distribution. IEEE Trans. Smart Grid 10(6), 6115–6125 (2019)
5. Ehsan, A., Yang, Q.: Active distribution system reinforcement planning with EV charging stations–part I: Uncertainty modeling and problem formulation. IEEE Trans. Sustainable Energy 11(2), 970–978 (2020)
6. Davidov, S., Pantoš, M.: Optimization model for charging infrastructure planning with electric power system reliability check. Energy 166, 886–894 (2019)
7. Zhang, H., Moura, S.J., Hu, Z., Qi, W., Song, Y.: A second-order cone programming model for planning PEV fast-charging stations. IEEE Trans. Power Syst. 33(3), 2763–2777 (2018)
8. Zhang, H., Moura, S.J., Hu, Z., Song, Y.: PEV fast-charging station siting and sizing on coupled transportation and power networks. IEEE Trans. Smart Grid 9(4), 2595–2605 (2018)
9. Zhou, B., Chen, G., Song, Q., Dong, Z.Y.: Robust chance-constrained programming approach for the planning of fast-charging stations in electrified transportation networks. Appl. Energy 262, 114480 (2020)
10. Kong, W., Luo, Y., Feng, G., Li, K., Peng, H.: Optimal location planning method of fast charging station for electric vehicles considering operators, drivers, vehicles, traffic flow and power grid. Energy 186, 115826 (2019)
11. Dong, X., Mu, Y., Jia, H., Wu, J., Yu, X.: Planning of fast EV charging stations on a round freeway. IEEE Trans. Sustainable Energy 7(4), 1452–1461 (2016)
12. Sadeghi-Barzani, P., Rajabi-Ghahnavieh, A., Kazemi-Karegar, H.: Optimal fast charging station placing and sizing. Appl. Energy 125, 289–299 (2014)
13. Zhang, A., Kang, J.E., Kwon, C.: Incorporating demand dynamics in multi-period capacitated fast-charging location planning for electric vehicles. Transport. Res. B: Meth. 103, 5–29 (2017)
14. Wang, Y., Shi, J., Wang, R., Liu, Z., Wang, L.: Siting and sizing of fast charging stations in highway network with budget constraint. Appl. Energy 228, 1255–1271 (2018)
15. Wu, F., Sioshansi, R.: A stochastic flow-capturing model to optimize the location of fast-charging stations with uncertain electric vehicle flows. Transp. Res. D Transp. Environ. 53, 354–376 (2017)
16. Zhang, H., Sheppard, C.J.R., Lipman, T.E., Zeng, T., Moura, S.J.: Charging infrastructure demands of shared-use autonomous electric vehicles in urban areas. Transp. Res. D Trans. Environ. 78, 102210 (2020)
17. Yang, Q., Sun, S., Deng, S., Zhao, Q., Zhou, M.: Optimal sizing of PEV fast charging stations with Markovian demand characterization. IEEE Trans. Smart Grid 10(4), 4457–4466 (2019)
18. Pahlavanhoseini, A., Sepasian, M.S.: Optimal planning of PEV fast charging stations using Nash bargaining theory. J. Storage Mater. 25, 100831 (2019)
19. Morro-Mello, I., Padilha-Feltrin, A., Melo, J.D., Calviño, A.: Fast charging stations placement methodology for electric taxis in urban zones. Energy 188, 116032 (2019)
20. Yang, J., Dong, J., Hu, L.: A data-driven optimization-based approach for siting and sizing of electric taxi charging stations. Transp. Res. Part C Emerg. Technol. 77, 462–477 (2017)
21. Mehrjerdi, H., Hemmati, R.: Electric vehicle charging station with multilevel charging infrastructure and hybrid solar-battery-diesel generation incorporating comfort of drivers. J. Storage Mater. 26, 100924 (2019)
22. Hung, D.Q., Dong, Z.Y., Trinh, H.: Determining the size of PHEV charging stations powered by commercial grid-integrated PV systems considering reactive power support. Appl. Energy 183, 160–169 (2016)
23. Tao, Y., Huang, M., Yang, L.: Data-driven optimized layout of battery electric vehicle charging infrastructure. Energy 150, 735–744 (2018)
24. Luo, L., Gu, W., Zhou, S., Huang, H., Gao, S., Han, J., et al.: Optimal planning of electric vehicle charging stations comprising multi-types of charging facilities. Appl. Energy 226, 1087–1099 (2018)
25. Graber, G., Calderaro, V., Mancarella, P., Galdi, V.: Two-stage stochastic sizing and packetized energy scheduling of BEV charging stations with quality of service constraints. Appl. Energy 260, 114262 (2020)
26. Erdinç, O., Taşcıkaraoğlu, A., Paterakis, N.G., Dursun, I., Sinim, M.C., Catalão, J.P.S.: Comprehensive optimization model for sizing and siting of dg units, ev charging stations, and energy storage systems. IEEE Trans. Smart Grid 9(4), 3871–3882 (2018)
27. Wang, S., Dong, Z.Y., Luo, F., Meng, K., Zhang, Y.: Stochastic collaborative planning of electric vehicle charging stations and power distribution system. IEEE Trans. Ind. Inf. 14(1), 321–331 (2018)
28. Luo, L., Gu, W., Wu, Z., Zhou, S.: Joint planning of distributed generation and electric vehicle charging stations considering real-time charging navigation. Appl. Energy 242, 1274–1284 (2019)
29. Awasthi, A., Venkitusamy, K., Padmanaban, S., Selvamuthukumaran, R., Blaabjerg, F., Singh, A.K.: Optimal planning of electric vehicle charging station at the distribution system using hybrid optimization algorithm. Energy 133, 70–78 (2017)
30. Pan, A., Zhao, T., Yu, H., Zhang, Y.: Deploying public charging stations for electric taxis: A charging demand simulation embedded approach. IEEE Access 7, 17412–17424 (2019)
31. Andrenacci, N., Ragona, R., Valenti, G.: A demand-side approach to the optimal deployment of electric vehicle charging stations in metropolitan areas. Appl. Energy 182, 39–46 (2016)

How to cite this article: Sengor, I., Erenoglu, A.K., Guldorum, H.C., Erdinc, O., Taşcıkaraoğlu, A., Taştan, İ.C., Büyük, A.F., Catalão, J.P.S.: Optimal sizing and siting of different types of EV charging stations in a real distribution system environment. IET Renew. Power Gener. 16, 3171–3183 (2022). https://doi.org/10.1049/rpg2.12566